

# Collective excitations in the Unitary Correlation Operator Method and relativistic QRPA studies of exotic nuclei

N. Paar, P. Papakonstantinou, H. Hergert, and R. Roth

*Institut für Kernphysik, Technische Universität Darmstadt,*

*Schlossgartenstrasse 9, D-64289 Darmstadt, Germany*

(Dated: July 1, 2005)

The collective excitation phenomena in atomic nuclei are studied in two different formulations of the Random Phase Approximation (RPA): (i) RPA based on correlated realistic nucleon-nucleon interactions constructed within the Unitary Correlation Operator Method (UCOM), and (ii) relativistic RPA (RRPA) derived from effective Lagrangians with density-dependent meson-exchange interactions. The former includes the dominant interaction-induced short-range central and tensor correlations by means of an unitary transformation. It is shown that UCOM-RPA correlations induced by collective nuclear vibrations recover a part of the residual long-range correlations that are not explicitly included in the UCOM Hartree-Fock ground state. Both RPA models are employed in studies of the isoscalar monopole resonance (ISGMR) in closed-shell nuclei across the nuclide chart, with an emphasis on the sensitivity of its properties on the constraints for the range of the UCOM correlation functions. Within the Relativistic Quasiparticle RPA (RQRPA) based on Relativistic Hartree-Bogoliubov model, the occurrence of pronounced low-lying dipole excitations is predicted in nuclei towards the proton drip-line. From the analysis of the transition densities and the structure of the RQRPA amplitudes, it is shown that these states correspond to the proton pygmy dipole resonance.

## I. INTRODUCTION

Among various theoretical approaches to nuclear structure, two pathways have been extensively pursued over the past decades: (i) models based on effective nuclear interactions constrained by the properties of nuclear matter and bulk properties of finite nuclei (e.g. Skyrme [1], Gogny [2], and relativistic models based on exchange of effective mesons [3]), and (ii) models which start from a realistic nucleon-nucleon (NN) interaction. Recently, several modern realistic NN interactions have been constructed, e.g., the Argonne V18 [5], the CD-Bonn [4], and chiral potentials [6], which reproduce the experimental NN phase-shifts with high accuracy. Within *ab initio* Green's function Monte Carlo [7] and no-core shell model calculations [8] of ground state properties and low-lying excitation spectra of light nuclei it was shown that realistic NN interactions, supplemented by a three-nucleon force, allow for a quantitative description of experimental data [9, 10].

Realistic NN interactions cannot be directly employed in a standard Hartree-Fock (HF) scheme due to the importance of interaction-induced correlations in the many-body state beyond the simple HF Slater determinant. Therefore, an effective, phase-shift equivalent interaction has to be derived by explicitly accounting for the dominant correlations. One way to tackle this issue is the Unitary Correlation Operator Method (UCOM) which describes the short-range central and tensor correlations by means of a unitary transformation [11–14]. The unitary transformation of the Hamiltonian including a realistic NN potential results in a correlated effective interaction well suited for the application with simple uncorrelated many-body states. An alternative method to derive phase-shift equivalent, low-momentum effective interactions is the  $V_{\text{low-}k}$  renormalization group approach [15].

Studies of collective excitation phenomena in atomic nuclei provide valuable insight into many properties of the underlying effective interactions employed in solving the nuclear many-body problem. In order to describe small-amplitude collective excitations within the UCOM framework, one can employ the random-phase approximation (RPA) [16], based on the HF single-nucleon basis. Since three-body interactions presently are not included, the results provide information on their importance for the understanding of collective nuclear excitations. The UCOM-RPA model can also be employed to evaluate the contributions of RPA correlations to the ground state energy which go beyond the mean-field picture [17]. In addition to the short-range correlations described explicitly by the unitary transformation,

the RPA ground state calculations allow for the inclusion of residual long-range correlations necessary to obtain a realistic, *ab initio*-type description of nuclei.

On the other side, models based on phenomenological nuclear interactions have been well established over the past decades, and have been very accurately tuned to the properties of finite nuclei. These models are nowadays successful not only in the region of stable nuclei, but also in the description of exotic nuclear structure and collective excitations in nuclei away from the valley of  $\beta$ -stability, both in the non-relativistic [18–20] and relativistic framework [21, 22]. Particularly interesting is the phenomenon of the pygmy dipole resonance in neutron-rich nuclei (PDR), indicating that the loosely bound neutrons might coherently oscillate against the approximately isospin-saturated proton-neutron core [23]. Very recently it has been shown that for proton rich nuclei in the lower region of the nuclide chart, one also could expect the appearance of a low-energy exotic collective mode, i.e. the proton PDR, when loosely-bound protons vibrate against the rest of the nucleons [24]. The experimental evidence about low-lying excitations in nuclei towards the drip-lines is still rather limited, and actually available only in light nuclei up to the oxygen isotopes [25]. The present article will summarize the recent progress in studies of low-lying excitations towards the proton drip-line within the Relativistic Quasiparticle RPA (RQRPA).

## II. THE HARTREE-FOCK MODEL IN THE UCOM FRAMEWORK

The UCOM approach aims at an explicit treatment of interaction-induced short-range central and tensor correlations in nuclei [11–14]. These correlations are imprinted into an uncorrelated many-body state  $|\Psi\rangle$  through a state-independent unitary transformation defined by the unitary operator  $C$ , resulting in a correlated state,  $|\hat{\Psi}\rangle = C |\Psi\rangle$ . Due to the unitarity of the correlation operator, matrix elements of an operator  $O$  in correlated many-body states are equal to those evaluated using the correlated operator  $\hat{O}$  and uncorrelated many-body states, i.e.

$$\langle \hat{\Psi} | O | \hat{\Psi}' \rangle = \langle \Psi | C^\dagger O C | \Psi' \rangle = \langle \Psi | \hat{O} | \Psi' \rangle. \quad (1)$$

The short-range central and tensor correlations are separately included via the unitary operators  $C_r$  and  $C_\Omega$ , respectively, and formulated as exponential functions of the two-body Hermitian generators  $g_r$  and  $g_\Omega$ . The operator form of the generators is motivated by the

basic physics of the two types of correlations we are going to describe explicitly.

The short-range central correlations are induced by the strong short-range repulsion in the central part of realistic NN interactions. This repulsive core prevents nucleons in a many-body system to approach each other closer than the characteristic size of the core. In the two-body density matrix these correlations are revealed through the depletion of the probability density for particle distances smaller than the core radius. In order to include these correlations into an uncorrelated many-body state, e.g., the Slater determinant of the Hartree-Fock approach, we perform a distance-dependent radial shift with respect to the relative coordinate of two-particles. The corresponding Hermitian generator  $g_r = \frac{1}{2}[s(\mathbf{r})\mathbf{q}_r + \mathbf{q}_r s(\mathbf{r})]$  contains the radial component of the relative momentum operator,  $\mathbf{q}_r$ , and a function  $s(r)$  which controls the distance-dependence of the shift. Implementation of the correlation operator in coordinate representation corresponds to a norm-conserving coordinate transformation  $\mathbf{r} \mapsto R_-(r)\frac{\mathbf{r}}{r}$  of the relative coordinate. The radial correlation function  $R_-(r)$  and its inverse  $R_+(r)$  are related to the shift function  $s(r)$  [13, 14].

For the following calculations the Argonne V18 (AV18) potential [5] is used. In practice, the correlation functions  $R_+(r)$  are parameterized and the optimal parameters are determined for each spin-isospin channel from an energy minimization in the two-body system [14]. Since the  $(S = 1, T = 1)$ -channel of the AV18 potential is purely repulsive, we employ a simple constraint on the range of the correlation function in this channel in order to avoid artificial long-range correlation functions. We have checked explicitly that the effect of variations of this constraint around the value that ensures the short-range of the correlation function, is negligible for all calculations presented here.

A second, equally important type of correlations is induced by the tensor part of the interaction [12]. They entangle the relative spatial orientation of two nucleons with their spin orientation. The generator  $g_\Omega$  has to describe an angular shift depending on the spin orientation. This is achieved by  $g_\Omega = \frac{3}{2}\vartheta(\mathbf{r})[(\boldsymbol{\sigma}_1 \cdot \mathbf{q}_\Omega)(\boldsymbol{\sigma}_2 \cdot \mathbf{r}) + (\boldsymbol{\sigma}_1 \cdot \mathbf{r})(\boldsymbol{\sigma}_2 \cdot \mathbf{q}_\Omega)]$ , where  $\mathbf{q}_\Omega = \mathbf{q} - \frac{\mathbf{r}}{r}\mathbf{q}_r$  [12]. As for the central correlations, the tensor correlation functions  $\vartheta(r)$ , which control the distance-dependence of the tensor correlator, are parameterized and determined by a two-body energy minimization. A characteristic of the tensor part of realistic NN interactions and thus of tensor correlations is their long range. We are not aiming at a description of long-range tensor correlations by the unitary transformation, since they are strongly system-dependent. In contrast to the deuteron, the long-range tensor correlations

in heavier nuclei will be largely screened. During the determination of the tensor correlators we therefore constrain the range or volume of  $\vartheta(r)$  given by

$$I_{\vartheta}^{(ST)} = \int dr r^2 \vartheta(r). \quad (2)$$

In the present study, we use the optimal tensor correlators for  $I_{\vartheta}^{(S=1,T=0)} = 0.07, 0.08,$  and  $0.09 \text{ fm}^3$  and investigate the effect on the global properties of collective excitation phenomena. No tensor correlator is employed in the  $(S = 1, T = 1)$ -channel, because there the tensor interaction is rather weak. It has been shown within no-core shell model calculations that for  $I_{\vartheta}^{(10)} = 0.09 \text{ fm}^3$  the experimental binding energies for  $A \leq 4$  are reproduced quite well [14].

The correlated operators constructed by the unitary transformation contain irreducible contributions, not only of one-body and two-body operators, but also higher  $n$ -body parts. This cluster expansion is truncated after the two-body level, leading to the so-called two-body approximation. In previous studies it has been verified that higher order contributions due to central correlations can be neglected in the description of nuclear structure properties [13]. For the tensor correlators the range constraint is important for the validity of the two-body approximation. The size of residual three-body and higher order contributions was estimated in [14].

Starting from the uncorrelated Hamiltonian for the  $A$ -body system, consisting of the kinetic energy operator and the bare AV18 potential, the central and tensor correlation operators are employed to construct the correlated Hamiltonian in the two-body approximation. Therein the one-body contributions come only from the uncorrelated kinetic energy, while two-body contributions arise from the correlated kinetic energy and the correlated potential, which together constitute the low-momentum correlated interaction  $V_{\text{UCOM}}$  [13, 14]. The  $V_{\text{UCOM}}$  interaction can directly be employed in the HF model to determine the single-particle wave functions and energies. By using the expansion in the harmonic oscillator basis, the HF equations are solved in a self-consistent way, with restrictions on the maximal value of the major shell quantum number  $N_{\text{max}} = 12$ , and maximal orbital angular momentum quantum number  $l_{\text{max}} = 8$ .

In Fig. 1 the UCOM-HF single-nucleon spectra are displayed for the case of  $^{40}\text{Ca}$ . The calculations are based on the correlated Argonne V18 interaction, with the constraint  $I_{\vartheta}^{(10)} = 0.09 \text{ fm}^3$  for the correlation volume of the tensor correlator, Eq. (2). The UCOM-HF energy levels

are compared with the HF spectrum obtained with the low-momentum NN potential  $V_{\text{low-}k}$  [26], with two standard phenomenological interactions in the nonrelativistic (Skyrme) [27] and relativistic (NL3) [28] framework, and with experimental levels [27]. The spectra obtained from the HF model based on realistic NN interactions appear distributed too wide in energy. In addition, the HF binding energies and radii are too small compared to the experimental values [13].

These deviations can be attributed to several missing pieces in the UCOM-HF description: (i) Long-range correlations are not covered by the unitary correlation operators and should be described by the model space, i.e. the available many-body states. The independent-particle states of the HF approach are clearly not able to do so and one has to go beyond the mean-field level. In the next section we are going to include long-range correlations due to collective vibrations, by means of RPA. (ii) Three-body forces, either genuine or induced by the unitary transformation, generally play a role for the quantitative description of nuclear structure. These are not included in the present study. Hence the results presented here will provide some information on their importance.

### III. RANDOM-PHASE APPROXIMATION BASED ON THE $V_{\text{UCOM}}$

The HF description of the nuclear ground state is to some extent oversimplified, and correlation effects going beyond mean-field should be included. Giant resonances may have some influence on the nuclear binding energies [17], and it is known that correlations due to surface vibrations have a considerable influence on the ground state densities [33]. In this section, we will employ an RPA model based on the UCOM Hamiltonian (UCOM-RPA) to evaluate the ground state correlations due to collective vibrations and to study the properties of such excitations themselves.

The UCOM-HF single-particle states are used for the construction of the  $ph$  configuration space for the RPA model. One of the standard approaches to derive the RPA equations is the equation of motion method with the quasiboson approximation [16], resulting in the eigenvalue problem formulated as a set of coupled equations for the forward and backward amplitudes,  $X_{ph}^{k, JM}$  and  $Y_{ph}^{k, JM}$  respectively,

$$\begin{pmatrix} A^J & B^J \\ B^{*J} & A^{*J} \end{pmatrix} \begin{pmatrix} X^{k, JM} \\ Y^{k, JM} \end{pmatrix} = \omega_k \begin{pmatrix} 1 & 0 \\ 0 & -1 \end{pmatrix} \begin{pmatrix} X^{k, JM} \\ Y^{k, JM} \end{pmatrix}. \quad (3)$$

The eigenvalues  $\omega_k$  correspond to RPA excitation energies and the RPA matrices are given by,

$$A_{php'h'}^J = \langle \phi | \left[ [A_{ph}^{JM}, H_{\text{UCOM}}], A_{p'h'}^{JM+} \right] | \phi \rangle \quad (4)$$

$$B_{php'h'}^J = -\langle \phi | \left[ [A_{ph}^{JM}, H_{\text{UCOM}}], (-1)^{J-M} A_{p'h'}^{J-M} \right] | \phi \rangle, \quad (5)$$

where the operator  $A_{ph}^{JM+}$  ( $A_{ph}^{JM}$ ) creates (annihilates) a  $ph$  state of angular momentum  $JM$ . We consistently use the intrinsic Hamiltonian  $H_{\text{UCOM}} = T - T_{\text{cm}} + V_{\text{UCOM}}$ , i.e., the center of mass contribution to the kinetic energy is subtracted on the operator level. The Coulomb interaction is included explicitly.

An essential property of the present model is that it is fully self-consistent, i.e. the same correlated realistic NN interaction  $V_{\text{UCOM}}$  is used in the HF equations that determine the single-particle basis, and in the RPA residual interaction entering the calculation of the RPA matrices. This essential property of our model ensures that RPA amplitudes do not contain spurious components associated with the center-of-mass translational motion. We have verified that the spurious  $1^-$  state is properly decoupled from the physical excitation states. We also have examined, for closed-shell nuclei across the nuclide chart, that the UCOM-RPA model essentially exhausts the isoscalar energy-weighted sum rules [16] with maximal discrepancies of  $\pm 3\%$ .

In the present study, the correlation energies are evaluated within the UCOM-RPA framework,

$$\delta E = - \sum_{k,J} (2J+1) \hbar \omega_k^J \sum_{ph} |Y_{ph}^{k,J}|^2, \quad (6)$$

by using the RPA eigenvalues  $\omega_k^J$ , and backward-going amplitudes  $Y_{ph}^{k,J}$ . Both, the natural  $\pi = (-1)^J$  and unnatural parity  $\pi = (-1)^{J+1}$  excitations are included, in the range of  $J^\pi = 0^\pm - 10^\pm$ . The HF binding energies together with RPA correlations due to collective excitations are shown in Fig. 2 for several closed-shell nuclei. The HF binding energies and UCOM-RPA correlations are calculated in a consistent way by using the correlated AV18 interaction for various ranges of the tensor correlator, constrained by  $I_\vartheta^{(10)} = 0.07, 0.08,$  and  $0.09 \text{ fm}^3$ . In general, the tensor correlator with longer range provides stronger binding both on the HF level and when the correlations are taken into account. In comparison with the experimental binding energies [34], the present model with full implementation of RPA correlations seems to favor the tensor correlator with shorter range. However, one

should keep in mind that the method used to evaluate the correlation energy, Eq. (6), is not free of over-counting [35] and therefore the correlation effects are overestimated. Within many-body perturbation theory or configuration interaction calculations, the longer ranged correlator provides a very good agreement with experimental binding energies for all nuclei in accord with the no-core shell model calculations discussed in [14].

By examining the electric transition strength, one can also study the properties of the correlated interaction  $V_{\text{UCOM}}$ . This is exemplified in Fig. 3, where the UCOM-RPA strength distributions, corresponding to the isoscalar giant monopole resonance (ISGMR) are displayed for the correlated AV18 interaction with different restrictions on the range of the tensor correlator,  $I_{\vartheta}^{(10)}=0.07, 0.08, \text{ and } 0.09 \text{ fm}^3$ . For the lighter nuclei  $^{16}\text{O}$ ,  $^{40}\text{Ca}$ , and  $^{48}\text{Ca}$ , the ISGMR is fragmented into two-three peaks, whereas for  $^{90}\text{Zr}$ ,  $^{132}\text{Sn}$ , and  $^{208}\text{Pb}$  the ISGMR is strongly collective, resulting essentially in a single peak. For a comparison, the monopole response is also calculated in the framework of relativistic RPA based on effective Lagrangian with density-dependent meson-nucleon vertex functions, with DD-ME1 interaction (more details are given in Sec. IV). In addition, the calculated ISGMR strength distributions are compared with the nonrelativistic RPA based on Woods-Saxon potential and G-matrix formalism [32], and with experimental data from  $(\alpha, \alpha)$  [29, 30] and  $(^3\text{He}, ^3\text{He})$  scattering [31]. One can observe that a decrease of the range of the tensor correlator systematically pushes the transition strength towards lower energies. In particular, by decreasing the range of the tensor correlator, i.e. its constraint  $I_{\vartheta}^{(10)}=0.09 \text{ fm}^3$  towards  $0.07 \text{ fm}^3$ , the excitation energy of ISGMR lowers by  $\approx 4 \text{ MeV}$ . This means that by varying the range of the tensor correlator, one can effectively control the impact of the missing correlations on the transition strength of ISGMR.

#### IV. PROTON PYGMY DIPOLE RESONANCE IN THE RELATIVISTIC QRPA

In this section we discuss recent developments regarding the response of nuclei far from  $\beta$ -stability. One of the major challenges in this region is the understanding of soft modes of excitations which involve loosely bound nucleons. In particular, in neutron-rich nuclei, nucleons from the neutron skin may give rise to a soft low-energy dipole mode known as the pygmy dipole resonance (PDR) [36–38]. The structure of nuclei on the proton-rich side is equally important for many aspects of the underlying many-body problem and effective

nuclear interactions. In a recent relativistic QRPA study, it has been predicted that in nuclei with proton excess one could expect the appearance of a proton PDR mode where loosely bound protons vibrate against the rest of the nucleons [24, 39]. The relativistic QRPA [21] is formulated in the canonical single-nucleon basis of the relativistic Hartree-Bogoliubov (RHB) model and is fully self-consistent. For the interaction in the particle-hole channel effective Lagrangians with nonlinear meson self-interactions or density-dependent meson-nucleon couplings are used [40], and pairing correlations are described by the pairing part of the finite-range Gogny interaction [2]. The parameters of the effective relativistic interaction have been adjusted to properties of nuclear matter and to binding energies, charge radii, and differences between neutron and proton radii of spherical nuclei [40]. In the small-amplitude limit, the RQRPA equations are derived from the equation of motion for the generalized nucleon density [21]. The RQRPA configuration space is constructed from standard ( $2qp$ ) pairs, but one also needs to include transitions to the unoccupied states from the Dirac sea [3, 42].

The RQRPA dipole strength distributions for  $N=20$  isotones, displayed in Fig. 4, are dominated by the isovector giant dipole resonances (GDR) at  $\approx 20$  MeV excitation energy. With the increase of the number of protons, low-lying dipole strength appears in the region below the GDR and, for  $^{44}\text{Cr}$  and  $^{46}\text{Fe}$ , a pronounced low-energy peak is found at  $\approx 10$  MeV excitation energy. In the lower panel of Fig. 4 we plot the proton and neutron transition densities for the peaks at 10.15 MeV in  $^{44}\text{Cr}$  and 9.44 MeV in  $^{46}\text{Fe}$ , and compare them with the transition densities of the GDR state at 18.78 MeV in  $^{46}\text{Fe}$ . Obviously the dynamics of the two low-energy peaks is very different from that of the isovector GDR: the proton and neutron transition densities are in phase in the nuclear interior and there is very small contribution from the neutrons in the surface region. By exploring the RQRPA amplitudes, we note that, rather than a single proton  $2qp$  excitation, the low-lying states are characterized by a superposition of a number of mainly proton  $2qp$  configurations. The low-lying state does not belong to statistical E1 excitations sitting on the tail of the GDR, but represents a fundamental mode of excitation: the proton electric pygmy dipole resonance (PDR).

## V. SUMMARY

In the present study, a fully self-consistent RPA model is constructed in the single-nucleon Hartree-Fock basis, by using correlated realistic NN interactions obtained within the UCOM framework. It is shown that the  $V_{\text{UCOM}}$  interaction generates a strongly collective ISGMR mode, whose energy is sensitive to the range of the tensor correlator. The UCOM-RPA correlations due to collective vibrations provide important contributions to the nuclear binding energies. In addition, by employing the fully self-consistent relativistic quasiparticle RPA, it is indicated that the nuclei towards the proton drip-line are characterized by the appearance of the proton pygmy dipole resonance, i.e. an exotic mode where loosely bound protons oscillate against the isospin-saturated proton-neutron core.

## ACKNOWLEDGMENTS

This work has been supported by the Deutsche Forschungsgemeinschaft (DFG) under contract SFB 634.

- 
- [1] D. Vautherin and D. M. Brink, *Phys. Rev. C* **5**, 626 (1972).
  - [2] J. Dechargé and D. Gogny, *Phys. Rev. C* **21**, 1568 (1980).
  - [3] D. Vretenar, A. V. Afanasjev, G. A. Lalazissis, and P. Ring, *Phys. Rep.* **409**, 101 (2005).
  - [4] R. Machleidt, *Phys. Rev. C* **63**, 024001 (2001).
  - [5] R. B. Wiringa, V. Stoks, and R. Schiavilla, *Phys. Rev. C* **51**, 38 (1995).
  - [6] D. R. Entem and R. Machleidt, *Phys. Lett. B* **524**, 93 (2002).
  - [7] S. C. Pieper, R. B. Wiringa, and J. Carlson, *Phys. Rev. C* **70**, 054325 (2004).
  - [8] P. Navrátil, J. P. Vary, and B. R. Barrett, *Phys. Rev. C* **62**, 054311 (2000).
  - [9] Steven C. Pieper, et al., *Phys. Rev. C* **64**, 014001 (2001).
  - [10] E. Epelbaum et al., *Phys. Rev. C* **66**, 064001 (2002).
  - [11] H. Feldmeier, T. Neff, R. Roth, J. Schnack, *Nucl. Phys. A* **632**, 61 (1998).
  - [12] T. Neff and H. Feldmeier, *Nucl. Phys. A* **713**, 311(2003).
  - [13] R. Roth, T. Neff, H. Hergert, and H. Feldmeier, *Nucl. Phys. A* **745**, 3 (2004).
  - [14] R. Roth, H. Hergert, P. Papakonstantinou, T. Neff, and H. Feldmeier, *nucl-th/0505080* (2005).

- [15] S. K. Bogner, T. T. S. Kuo, A. Schwenk, Phys. Rep. **386**, 1 (2003).
- [16] D. J. Rowe, Nuclear Collective Motion, (Methuen and Co. LTD., London 1970).
- [17] P.-G. Reinhard and J. Friedrich, Z. Phys. A **321**, 619 (1985).
- [18] M. Matsuo, Nucl. Phys. A **696**, 371 (2001).
- [19] J. Terasaki, J. Engel, M. Bender, J. Dobaczewski, W. Nazarewicz, and M. Stoitsov, Phys. Rev. C **71**, 034310 (2005).
- [20] D. Sarchi, P. F. Bortignon, and G. Coló, Phys. Lett. B **601**, 27 (2004).
- [21] N. Paar, P. Ring, T. Nikšić, and D. Vretenar, Phys. Rev. C **67**, 034312 (2003).
- [22] L. G. Cao and Z. Y. Ma, Phys. Rev. C **71**, 034305 (2005).
- [23] D. Vretenar, N. Paar, P. Ring, and G. A. Lalazissis Nucl. Phys. A **692**, 496 (2001).
- [24] N. Paar, D. Vretenar, and P. Ring, Phys. Rev. Lett. **94**, 182501 (2005).
- [25] A. Leistenschneider et al., Phys. Rev. Lett. **86**, 5442 (2001).
- [26] L. Coraggio et al., Phys. Rev. C **68**, 034320 (2003).
- [27] V. I. Isakov et al., Eur. Phys. J. A **14**, 29 (2002).
- [28] G.A. Lalazissis, J. König, and P. Ring, Phys. Rev. C **55**, 540 (1997).
- [29] D. H. Youngblood, H. L. Clark, and Y.-W. Lui, Phys. Rev. Lett. **82**, 691 (1999).
- [30] S. Shlomo and D. H. Youngblood, Phys. Rev. C **47**, 529 (1993).
- [31] M. M. Sharma and M. N. Harakeh, Phys. Rev. C **38**, 2562 (1988).
- [32] S. Drożdż, S. Nishizaki, J. Speth, and J. Wambach, Phys. Rep. **197**, 1 (1990).
- [33] H. Esbensen and G. F. Bertsch, Phys. Rev. C **28**, 355 (1983).
- [34] G. Audi and A. Wapstra, Nucl. Phys. A **595**, 409 (1995).
- [35] N. Ullah and D. J. Rowe, Phys. Rev. **188**, 1640 (1969).
- [36] Y. Suzuki, K. Ikeda, and H. Sato, Prog. Theor. Phys. **83**, 180 (1990).
- [37] N. Paar, T. Nikšić, D. Vretenar, and P. Ring, Phys. Lett. B **606**, 288 (2005).
- [38] N. Paar, T. Nikšić, D. Vretenar, and P. Ring, Int. J. Mod. Phys. E **14**, 1 (2005).
- [39] N. Paar, P. Papakonstantinou, V. Yu. Ponomarev, and J. Wambach, nucl-th/0506010 (2005).
- [40] T. Nikšić, D. Vretenar, P. Finelli, and P. Ring, Phys. Rev. C **66**, 024306 (2002).
- [41] T. Nikšić, D. Vretenar, and P. Ring, Phys. Rev. C **66**, 064302 (2002).
- [42] N. Paar, T. Nikšić, D. Vretenar, and P. Ring, Phys. Rev. C **69**, 054303 (2004).

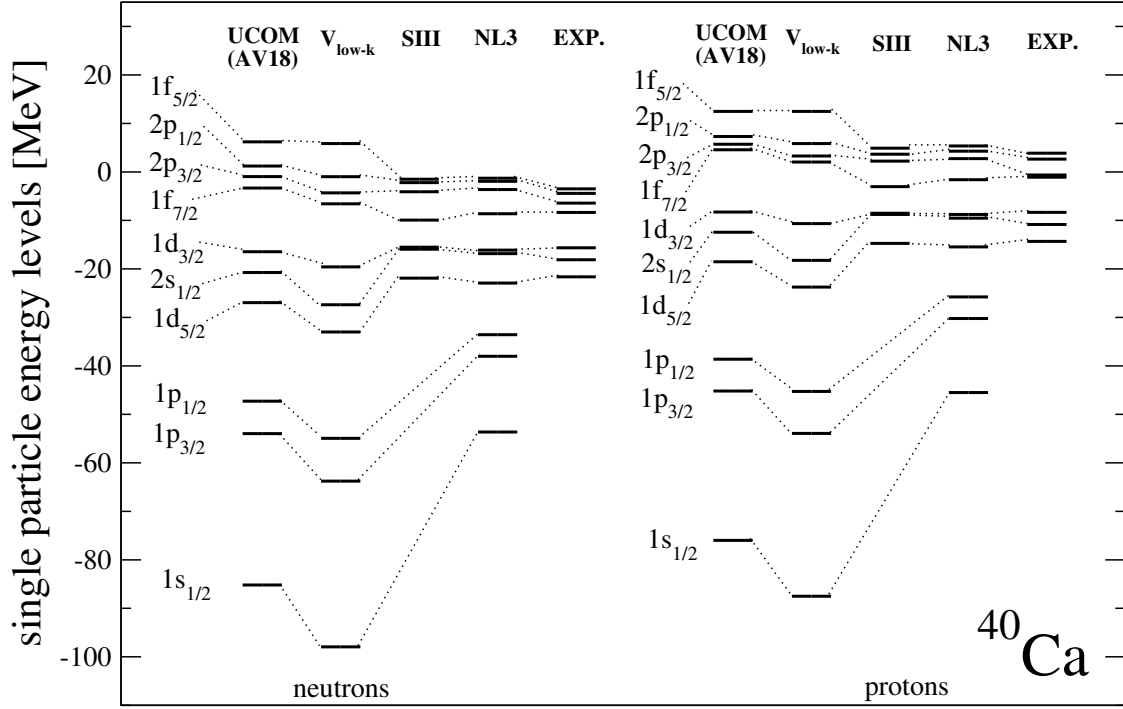


FIG. 1: The UCOM-HF neutron and proton single particle spectrum for  $^{40}\text{Ca}$ , along with the corresponding spectra from the HF model based on the low-momentum NN potential  $V_{\text{low-k}}$  [26], HF with SIII Skyrme-type interaction [27], relativistic mean field theory with NL3 effective interaction [28], and experimental spectrum [27]. The UCOM-HF calculations are based on the correlated Argonne V18 interaction ( $I_{\theta}^{(10)}=0.09 \text{ fm}^3$ ).

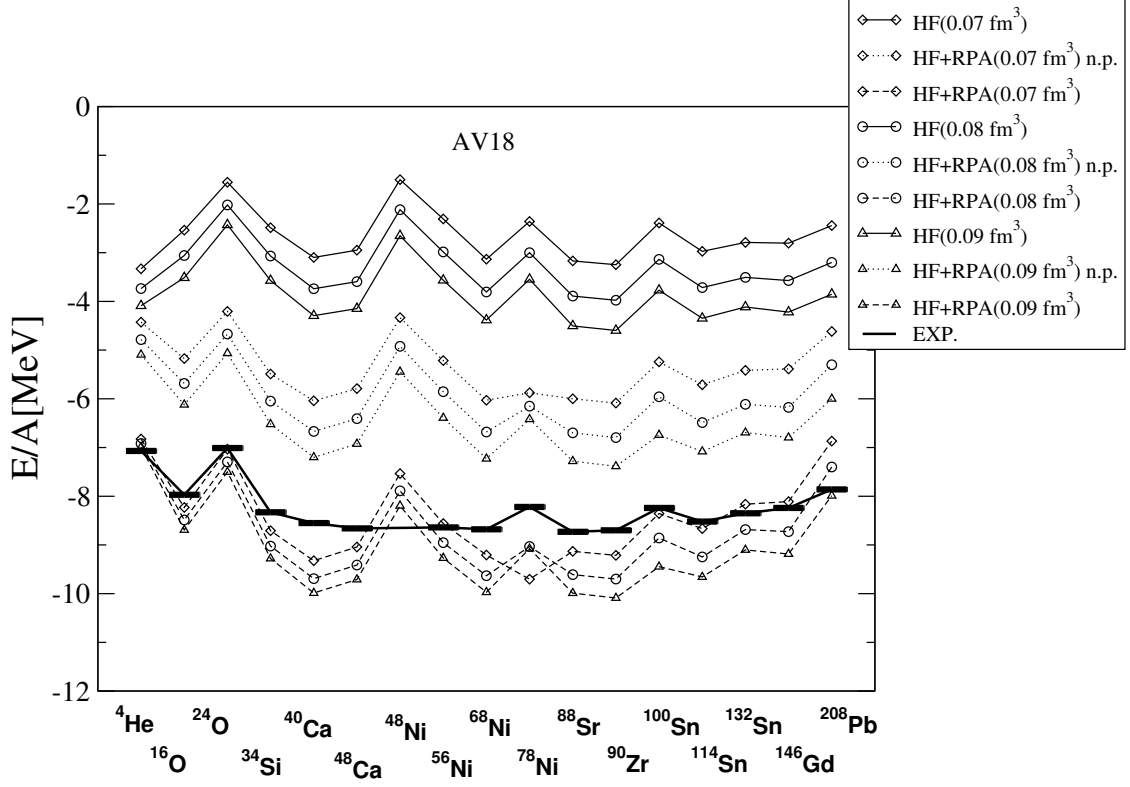


FIG. 2: The Hartree-Fock binding energies for a series of closed-shell nuclei, in comparison with the corrected binding energies due to UCOM-RPA correlations from collective vibrations, and experimental data [34]. The binding energies with the full correction (dashed line) and only with natural parity excitations (dotted line, n.p.) are separately displayed. Both the Hartree-Fock and RPA calculations are based on the correlated Argonne V18 interaction with various ranges of the tensor correlator ( $I_{\rho}^{(10)}=0.07, 0.08, \text{ and } 0.09 \text{ fm}^3$ ).

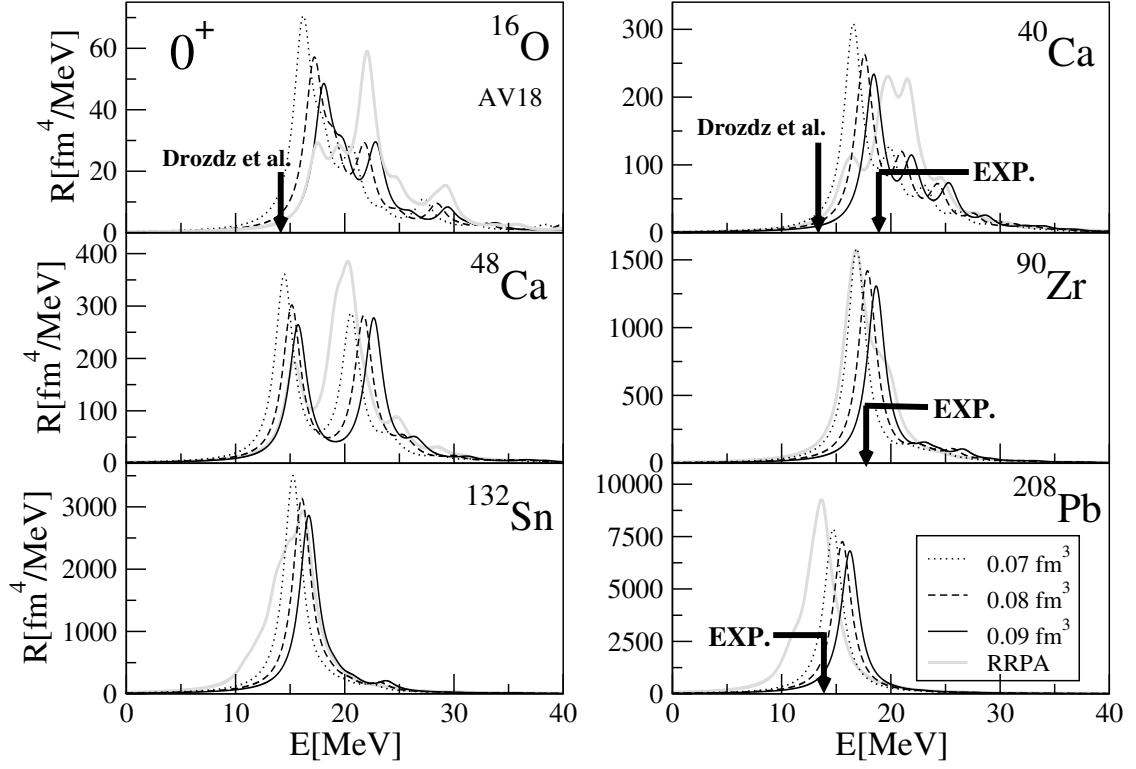


FIG. 3: The UCOM-RPA monopole transition strength distributions for the correlated Argonne V18 interaction, using different restrictions on the range of the tensor correlator ( $I_{\rho}^{(10)}=0.07, 0.08,$  and  $0.09 \text{ fm}^3$ ). The grey lines correspond to the monopole response from the relativistic RPA, based on the effective Lagrangian with density-dependent meson-nucleon couplings [40], with DD-ME1 parameterization [41]. The ISGMR centroid energies obtained from nonrelativistic (Drozd et al.) calculations [32] and experimental data [29–31] are denoted by arrows.

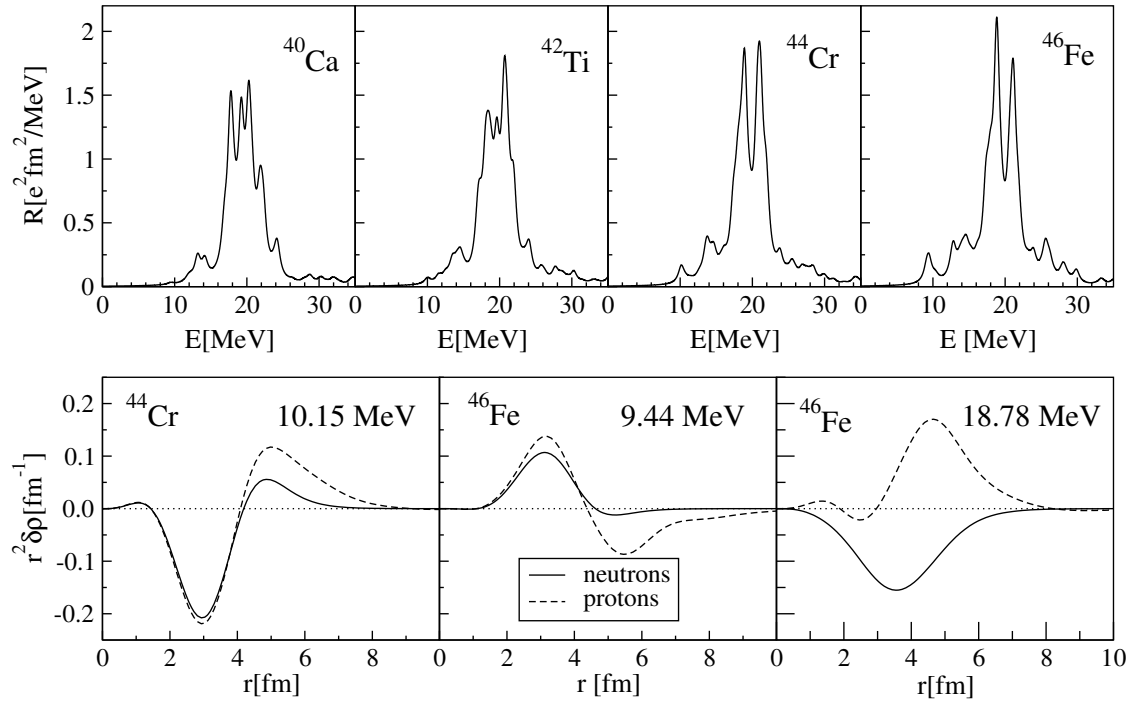


FIG. 4: The RHB+RQRPA isovector dipole strength distributions in the  $N=20$  isotones, calculated with the DD-ME1 effective interaction. For  $^{44}\text{Cr}$  and  $^{46}\text{Fe}$  the proton and neutron transition densities for the main peak in the low-energy region are displayed in the lower panel and, for  $^{46}\text{Fe}$ , the transition densities for the main GDR peak.